Magnetic Clusters

Deutsche Ausgabe: DOI: 10.1002/ange.201601199
Internationale Ausgabe: DOI: 10.1002/anie.201601199

Magnetic Properties of a Single-Molecule Lanthanide–Transition-Metal Compound Containing 52 Gadolinium and 56 Nickel Atoms

Da-Peng Liu[+], Xin-Ping Lin[+], Hui Zhang[+], Xiu-Ying Zheng, Gui-Lin Zhuang, Xiang-Jian Kong,* La-Sheng Long,* and Lan-Sun Zheng*

Dedicated to Professor T. C. W. Mak on the occasion of his 80th birthday

Abstract: *Monodisperse metal clusters provide a unique platform for investigating magnetic exchange within molecular magnets. Herein, the core–shell structure of the monodisperse molecule magnet of $[Gd_{52}Ni_{56}(IDA)_{48}(OH)_{154}(H_2O)_{38}]@SiO_2$ (**1a**@SiO_2) was prepared by encapsulating one high-nuclearity lanthanide–transition-metal compound of $[Gd_{52}Ni_{56}(IDA)_{48}(OH)_{154}(H_2O)_{38}]\cdot(NO_3)_{18}\cdot 164\,H_2O$ (**1**) (IDA = iminodiacetate) into one silica nanosphere through a facile one-pot microemulsion method. **1a**@SiO_2 was characterized using transmission electron microscopy, N_2 adsorption–desorption isotherms, and inductively coupled plasma-atomic emission spectrometry. Magnetic investigation of **1** and **1a** revealed $J_1 = 0.25\ cm^{-1}$, $J_2 = -0.060\ cm^{-1}$, $J_3 = -0.22\ cm^{-1}$, $J_4 = -8.63\ cm^{-1}$, $g = 1.95$, and $zJ = -2.0\times10^{-3}\ cm^{-1}$ for **1**, and $J_1 = 0.26\ cm^{-1}$, $J_2 = -0.065\ cm^{-1}$, $J_3 = -0.23\ cm^{-1}$, $J_4 = -8.40\ cm^{-1}$ $g = 1.99$, and $zJ = 0.000\ cm^{-1}$ for **1a**@SiO_2. The $zJ = 0$ in **1a**@SiO_2 suggests that weak antiferromagnetic coupling between the compounds is shielded by silica nanospheres.*

Significant research interest has been devoted to nanosized, single-molecule metal clusters because of their distinct chemical and physical properties.[1–5] For example, individual single-molecule magnets (SMMs) Mn_{12} have been dispersed on the surface of a polymeric thin film,[6] the surface of Au(111),[7] or incorporated into metal–organic frameworks (MOF)[8a] or carbon nanotubes.[8b–c] Sessoli and co-workers found that Fe_4 SMMs retain magnetic hysteresis at gold surfaces.[9] These individual SMMs have potential applications in information storage devices and quantum computing.[6–9] In an effort to isolate such single-molecule metal clusters, several synthetic strategies have been developed.[6–10]

Featuring 3d and 4f elements in the same molecule, and often in nanoscale, high-nuclearity lanthanide–transition-metal compounds possess unique magnetic properties that are not available in their mononuclear species or bulk samples.[11] In the past decades, significant effort has been made to reveal the magnetic interactions in the high-nuclearity lanthanide–transition-metal compounds.[12–14] A theoretical study of the magnetic interaction between the metal ions in the high-nuclearity lanthanide–transition-metal compounds remains rare.[15] Experimental investigation on the magnetic interaction of the high-nuclearity lanthanide–transition-metal compounds is invariably based on their bulk solid-state samples. To the best of our knowledge, there is no precedent to study the magnetic interaction in the single-molecule high-nuclearity lanthanide–transition-metal compounds, although the magnetic interaction in the compounds is not only involved in metal–metal magnetic exchanges within the compounds, but also the strength of magnetic interactions between the compounds.

Here, we report a new simple methodology to study the magnetic interaction of individual molecule compounds by encapsulating individual molecule compounds into one SiO_2 nanosphere, forming a hybrid core–shell nanoparticle cluster@SiO_2. The fabricated hybrid core–shell nanoparticle can enhance the stability and nanoscale manipulation by overcoming the chemical instability of the compound on the surfaces[9b] and can isolate the magnetic compound, preventing noisy intercluster interactions. The integrated core–shell cluster encapsulated in a SiO_2 nanoparticle provides a tunable platform for investigating individual molecular magnetism from an experimental and theoretical point of view.

The compound, formulated as $[Gd_{52}Ni_{56}(IDA)_{48}(OH)_{154}(H_2O)_{38}]\cdot(NO_3)_{18}\cdot 164\,H_2O$ (**1**) (IDA = iminodiacetate), was prepared through the refluxing reaction of $Ni(NO_3)_2\cdot 6\,H_2O$, $Ln(NO_3)_3\cdot 6\,H_2O$, and iminodiacetic acid (see the Supporting Information; IDA = iminodiacetate). Single-crystal structure analysis revealed that **1** contains $52\,Gd^{3+}$, $56\,Ni^{2+}$, 48 IDA, $154\,OH^-$, 38 coordinated water molecules, $18\,NO_3^-$, and approximately 164 guest water molecules. Structurally, the cationic cluster of $[Gd_{52}Ni_{56}(IDA)_{48}(OH)_{154}(H_2O)_{38}]^{18+}$ (**1a**)

[*] D.-P. Liu,[+] X.-P. Lin,[+] H. Zhang,[+] X.-Y. Zheng, Prof. Dr. X.-J. Kong, Prof. Dr. L.-S. Long, Prof. Dr. L.-S. Zheng
Collaborative Innovation Center of Chemistry for Energy Materials
State Key Laboratory of Physical Chemistry of Solid Surface and Department of Chemistry, College of Chemistry and Chemical Engineering
Xiamen University
Xiamen, 361005 (China)
E-mail: xjkong@xmu.edu.cn
lslong@xmu.edu.cn
Dr. G.-L. Zhuang
College of Chemical Engineering
Zhejiang University of Technology
Hangzhou 310032 (China)
E-mail: glzhuang@zjut.edu.cn
[+] These authors contributed equally to this work.

Supporting information for this article, including the crystal data and structure of **1**, DLS and EDS measurements of **1**, and an introduction of Quantum Monte Carlo Simulation, can be found under http://dx.doi.org/10.1002/anie.201601199.

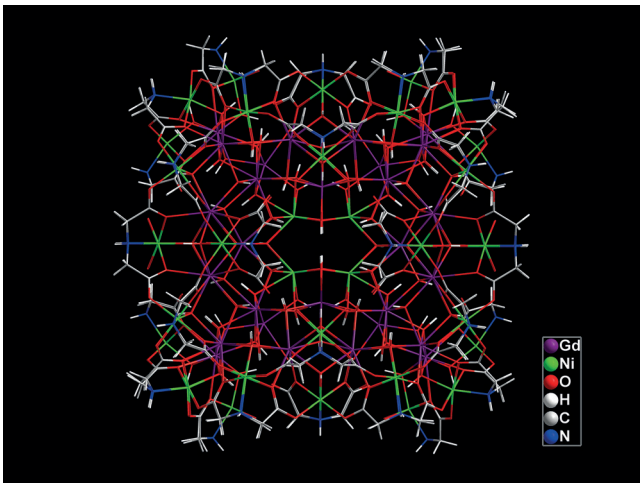

Figure 1. The structure of the cation cluster of $[Gd_{52}Ni_{56}(IDA)_{48}(OH)_{154}(H_2O)_{38}]^{18+}$.

can be viewed as two Gd^{III} and six CO_3^{2-} in the four-shell nesting doll-like structure reported previously[11] replaced by two Ni^{II} and twelve OH^- groups, respectively (Figure 1).

The innermost shell contains $8\,Ni^{2+}$ ions occupying the vertices of the cube. The $8\,Ni^{2+}$ ions are connected by 10 μ_2-OH, 2 μ_2-OH_2, and 12 μ_3-OH groups. The coordination sphere of each of the eight Ni^{2+} ions is completed by three additional μ_3-OH groups, which connect the vertex Gd^{3+} and three edge Gd^{3+} ions in shell 2. Shell 2 of Gd_{20} features a roughly cubic framework, with eight Gd^{3+} ions at the vertices and the remaining 12 Gd^{3+} ions in the middle of the 12 cube edges. Nine μ_3-OH groups form the coordination sphere for each of the vertex-occupying Gd^{3+} ions. Each pair of neighboring metals is connected by a pair of μ_3-OH groups, except for the two vertex metals with 3 μ_3-OH groups. Shell 3 contains $32\,Gd^{3+}$ ions, which can be viewed as a cubic framework with dimensions of $12\times12\times12$ Å^3. There are two Gd^{3+} ions on each edge of shell 3, which differs from shell 2 with one Gd^{3+} ion. Three μ_3-OH groups exist between each pair of the edge Gd^{3+} ions: one μ_3-OH group bridges an edge Gd^{3+} in shell 2 and the other two connect two separate Ni^{2+} ions of shell 4. Two μ_3-OH groups link the vertex Gd^{3+} ion and each of its neighbors. Shell 4 of Ni_{48} can be viewed as a truncated cube ($17\times17\times17$ Å^3) with each of its vertices being a triangle of Ni^{2+} ions, and each cube edge contains two Ni^{2+} ions. All Ni^{2+} ions are situated in a distorted octahedral environment, and each of the Ni^{2+} in the vertex-occupying triangle is connected to four neighboring Ni^{2+} ions. Notably, 144 triply bridging hydroxo groups connect the adjacent shells, forming a highly compact, brucite-like core structure (Figures S1–S3). The Gd···Gd, Gd···Ni and Ni···Ni distances are 3.4826(10)–4.0406(12) Å, 3.4860(16)–3.8168(24) Å, and 3.6689–5.3509(23) Å, respectively, all comparable to the corresponding values in the $Gd_{54}Ni_{54}$ cluster.[11]

Because **1** easily dissolves in water, the stability of **1** in aqueous solution was investigated. As shown in Figure 2a, the small angle X-ray scattering (SAXS) measurement of **1** reveals that the maximum value of the hydrodynamic diameter for **1a** is approximately 2.6 nm at pH 7 and 10, close

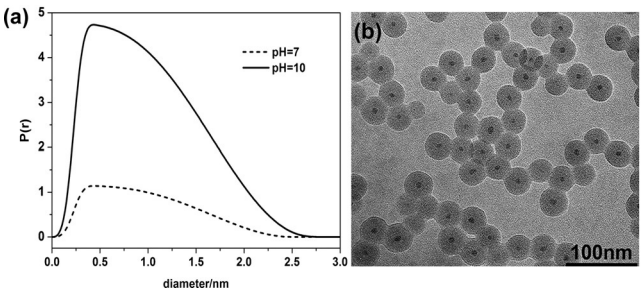

Figure 2. a) SAXS plots of **1** at pH 7 and pH 10 and b) TEM images of **1a**@SiO_2.

to the value of 2.8 nm obtained from the crystal data. Consistently, the dynamic light-scattering (DLS) result shows that the mean hydrodynamic diameter of **1a** is approximately 2.8 nm (Figure S4). These results indicate that **1a** is stable in aqua solution in the pH range from 7 to 10. Because **1a** is stable in solution and possesses a highly positive charge, it will be separated as far as possible in aqueous solution because of the charge repulsion between the compounds. Thus, **1a** can be encapsulated into silica nanospheres. Monodisperse **1a**@SiO_2 was successfully obtained through a microemulsion method. As shown in Figure 2b, the transmission electron microscopy (TEM) images show that the diameter of the **1a**@SiO_2 nanosphere is 27 ± 2 nm, whereas the cation compound size in the pore of the silica nanosphere is approximately 4 ± 1 nm.

The Brunauer–Emmett–Teller (BET) measurement of **1a**@SiO_2 shows that the average pore diameter is 25 nm (Figure S5, inset). Based on the BET curves, the surface area of **1a**@SiO_2 is approximately 162.38 m^2g^{-1}. This value is significantly larger than that of 90.91 m^2g^{-1} calculated for a perfectly smooth sphere of 25 nm in diameter with a density of 2.2 gcm^{-3} for silica. The significant difference in the surface area of **1a**@SiO_2 between the experimental and calculated is attributed to the surface absorption in the hysteresis loop between adsorption and absorption (Figure S5).

To confirm that **1a** was encapsulated in the pore of the silica nanospheres, energy dispersive spectrometry (EDS) analysis was performed on the **1a**@SiO_2 samples (Figure S6). As shown in Figure S5, Si, O, Gd, and Ni are present in **1a**@SiO_2. The inductively coupled plasma-atomic emission spectrometer (ICP-AES) result indicates that the contents of Ni^{2+} and Gd^{3+} in **1a**@SiO_2 are 0.52 and 1.39 %, respectively. Based on these data, the ratio of Ni to Gd in **1a**@SiO_2 is 1.01, consistent with that of 1.07 obtained from the crystal structure of **1**.[26] These results further confirm the presence of the compound in the silica nanosphere.

The variable-temperature magnetic susceptibilities of **1** and **1a**@SiO_2 under an external field of 1000 Oe are shown in Figure 3. At 300 K, the $\chi_M T$ values for **1** and **1a**@SiO_2 are 452.5 and 463.6 cm^3Kmol^{-1}, respectively. The $\chi_M T$ value for **1** is slightly smaller than the calculated value of 465.73 cm^3Kmol^{-1} for 56 uncorrelated Ni^{2+} ions (55.97 cm^3Kmol^{-1} for $S=1$, $g=2.00$) and 52 uncorrelated Gd^{3+} ions ($S=7/2$, $g=2$; 409.76 cm^3Kmol^{-1}),[16] whereas the

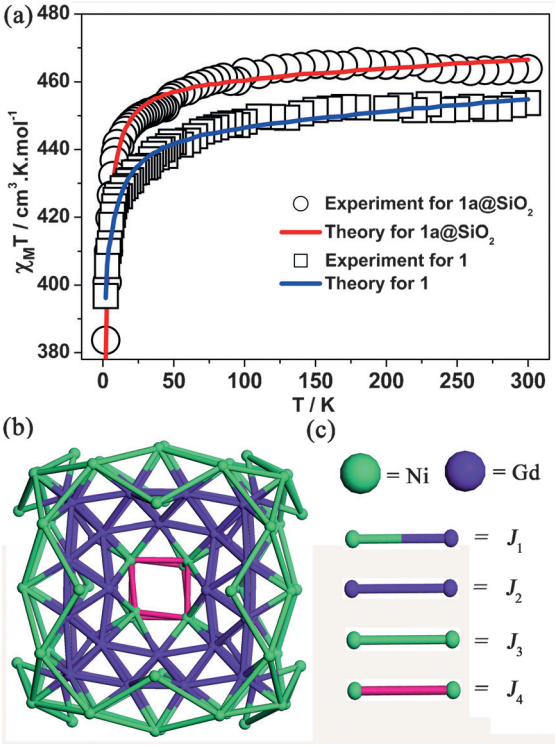

Figure 3. a) Experiment plot of $\chi_M T$ vs. T of **1a**@SiO_2 (○) and pristine **1** (□) under an external field of 1000 Oe; fitting curves (solid line) for $\chi_M T$ versus T for **1a**@SiO_2 (red) and **1** (blue); b–c) sketch of 52 Gd^{3+} ions and 56 Ni^{2+} ions in **1**.

$\chi_M T$ value for **1a**@SiO_2 is consistent with the calculated value. With decreasing temperature, the $\chi_M T$ values for **1** and **1a**@SiO_2 decrease gradually and reach 400.0 $cm^3 K mol^{-1}$ for **1** and 383.6 $cm^3 K mol^{-1}$ for **1a**@SiO_2 at 2 K, indicating the presence of antiferromagnetic interactions and crystal-field effects in **1** and **1a**@SiO_2. Fitting the data over the temperature range 2–300 K with the Curie–Weiss equation gives $C =$ 458.7 and $\theta = -1.29$ K for **1** and $C = 465.1$ and $\theta = -0.767$ K for **1a**@SiO_2. Moreover, the magnetization values of 482 N μ_B for **1** and 467 N μ_B for **1a**@SiO_2 at 7 T are similar to the theoretical saturation value of 476 N μ_B, suggesting the lack of significant anisotropy and low-lying excited states. The magnetocaloric properties of **1** and **1**a@SiO_2 were studied because of the isotropic Gd^{III} centres. The observed maximum value ΔS_m of **1** is 40.5 J $kg^{-1} K^{-1}$ at 3 K for $\Delta H = 7$ T, which is smaller than the calculated value of 52.4 J $kg^{-1} K^{-1}$ (146.9 R for the spins of 52 uncorrelated Gd^{3+} and 56 uncorrelated Ni^{2+}). The maximum ΔS_m of **1**a@SiO_2 (subtracting the background of SiO_2) is 44.6 J $kg^{-1} K^{-1}$ at 4 K for $\Delta H = 7$ T. Compared to compound **1**, the maximum value for **1**a@SiO_2 is increased by 10%, which may be attributed to the lack of intercluster interactions in **1**a@SiO_2.

The simulations of the magnetic interaction between **1** and **1a**@SiO_2 were performed to probe the different couplings. The magnetic interaction in **1** and **1a**@SiO_2 is involved four different magnetic couplings, i.e., Gd···Ni (J_1) in the bridge of μ_3-OH^- and/or μ_2-O of the carboxylate, Gd···Gd (J_2) in the bridge of μ_3-OH^-, Ni···Ni (J_3) in the bridge of *syn-anti* carboxylate and Ni···Ni (J_4) in the bridge of μ_3-OH^-, and the whole cluster is involved in 328 connections, that is, 128J_1, 116J_2, 72J_3, and 12J_4. It is impossible to simulate the magnetic interaction in such a complicated system through traditional Irreducible tensor operators (ITO)[17] and density functional theory (DFT)[18] method.

Thus, based on the Heisenberg Hamiltonian equation [Eq. (1)],[19] we developed a quantum Monte Carlo (QMC)

$$H = -\sum_{i=1}^{n=4} J_i \left(\sum_{j=1,k=1}^{j<109,k<109} S_{ij} S_{ik} \right) \quad (1)$$

magnetic fitting program (Supporting Information) by embedding the directed loop code[20] of ALPS software[21] to reveal the differences in the magnetic interactions between **1** and **1a**@SiO_2. Because of the effect of the large paramagnetic centers in the compound, the temperature-independent paramagnetism (TIP) parameter was taken into account. The zJ parameter is used to describe weak interactions of the inter-compounds.

According to the principle of the least reliability factor ($\Sigma[(\chi_M T)_{obs} - (\chi_M T)_{calcd}]^2 / \Sigma[(\chi_M T)_{obs}]^2$), the obtained best parameters are: $J_1 = 0.25$ cm^{-1}, $J_2 = -0.060$ cm^{-1}, $J_3 = -0.22$ cm^{-1}, $J_4 = -8.63$ cm^{-1}, $g = 1.95$, $zJ = -2.0 \times 10^{-3}$ cm^{-1}, TIP $= 4.40 \times 10^{-4}$ $cm^3 mol^{-1}$, and $R = 3.2 \times 10^{-5}$ for **1**, and $J_1 = 0.26$ cm^{-1}, $J_2 = -0.065$ cm^{-1}, $J_3 = -0.23$ cm^{-1}, $J_4 = -8.40$ cm^{-1} $g = 1.99$, $zJ = 0.000$ cm^{-1}, TIP $= 2.0 \times 10^{-4}$ $cm^3 mol^{-1}$, and $R = 2.4 \times 10^{-5}$ for **1a**@SiO_2. Thus, we can draw four conclusions: 1) the positive values of J_1 for **1** and **1a**@SiO_2 reveal weak ferromagnetic coupling between Gd^{3+} and Ni^{2+}, consistent with the experimental result in $GdNi_6$[22a] and the DFT computational results of Rajaraman and Ruiz.[22b,c] The weak antiferromagnetic exchange of Gd···Gd (J_2) is dominated by the average bond angle of Gd-O(H)-Gd (108.1°), in agreement with the experimental result of $Gd_{24}Zn_4$[23a] and the calculated result of Hughbanks.[23b] Although the J_2 value of is very small, the interaction of Gd···Gd cannot be ignored. In addition, the *syn-anti* coordination mode of carboxylate renders the weak antiferromagnetic coupling trait of Ni···Ni (-0.22 cm^{-1} for **1** and -0.23 cm^{-1} for **1a**@SiO_2), and the μ_3-OH^- bridge causes the antiferromagnetic character of Ni···Ni (-8.63 cm^{-1} for **1**, -8.40 cm^{-1} for **1a**@SiO_2), which is compatible with the experimental result of $GdNi_6$.[22a] Notably, the angle (115.2–125.8°) of Ni-O-Ni plays a critical role in the magnetic interaction.[24] 2) The four coupling parameters (J_1, J_2, J_3 and J_4) in **1a**@SiO_2 are similar to those in **1**, which indicates that the framework of **1** is maintained in **1a**@SiO_2, even after encapsulation in silica nanospheres, consistent with the TEM images of **1a**@SiO_2. 3) The $zJ = 0$ in **1a**@SiO_2 suggests that weak antiferromagnetic coupling (-2.0×10^{-3} cm^{-1}) of inter-compounds is shielded by diamagnetic silica nanospheres, further confirming that each silica nanosphere only encapsulates one compound. 4) The value of the Landé factor g in **1a**@SiO_2 is slightly larger than that in **1**, which may be attributed to the average g-tensor of the 3d shell in Ni^{2+} ions and the 5d shell in Gd^{3+} ions being influenced by the confining effect of the silica nanospheres.[25]

In summary, the single-molecule lanthanide–transition-metal compound of **1a**@SiO_2 has successfully been prepared

through a facile one-pot microemulsion method, and its magnetic properties have been investigated experimentally and theoretically. Because there is no precedent for analyzing the magnetic interaction of the single-molecule high-nuclearity lanthanide–transition-metal compound, the present study represents the first example of an experimental investigation of the magnetic interaction of the single-molecule high-nuclearity lanthanide–transition-metal compound and the first theoretical study on the magnetic interaction of the single-molecule high-nuclearity lanthanide–transition-metal compound. Thus, the present study is beneficial to our understanding of the magnetic interactions in high-nuclearity, lanthanide–transition-metal compounds.

Experimental Section

Synthesis of **1**: A mixture of $Ni(NO_3)_2{\cdot}6H_2O$(1.163 g, 4 mmol), $Gd(NO_3)_3{\cdot}6H_2O$ (0.902 g, 2.00 mmol), and iminodiacetic acid (0.266 g, 2.00 mmol) was dissolved in deionized water (15.0 mL); then, fresh NaOH was added dropwise to the mixture until the point of incipient but permanent precipitation. The mixture was refluxed for two hours and then filtered. Block-shaped green crystals of **1** were obtained at a 40% yield after the filtrate was stored at room temperature for **1** week.

Synthesis of **1a**@SiO_2: 4.7 mL of heptane as an oil phase was mixed with 1.5 mL of Brij ®30(surfactant) in a bottle with rapid stirring. Then, 160 μL of aqueous **1** (18 mg mL^{-1}) was slowly added to the mixture with stirring for 10 minutes. Then, 130 μL of ammonia was slowly added to the solution. After stirring for 30 minutes, 200 μL of the silica precursor TEOS (tetraethyl orthosilicate) was added slowly. The solution was stirred for 24 h and was then destabilized with 3 mL ethanol. The core–shell nanoparticles of **1a**@ silica were obtained at a 75% yield (based on **1**) after washing with heptane and ethanol.

Acknowledgements

This work was supported by the the Ministry of Science and Technology of China under 973 project (grant numbers 2012CB821704 and 2014CB845601) and by the National Natural Science Foundation of China (grant numbers 21422106, 21371144, 21431005, and 21390391). We thank N. F. Zheng, X. L. Fang, J. H. Gao, and Y. Z. Zheng for experimental help and discussions.

Keywords: core–shell nanoparticles · lanthanide–transition-metal compounds · magnetic properties · silica · single molecules

How to cite: *Angew. Chem. Int. Ed.* **2016**, *55*, 4532–4536
Angew. Chem. **2016**, *128*, 4608–4612

[1] K. Okamoto, R. Akiyama, H. Yoshida, T. Yoshida, S. Kobayashi, *J. Am. Chem. Soc.* **2005**, *127*, 2125.
[2] T. Mitsudome, K. Nose, K. Mori, T. Mizugaki, K. Ebitani, K. Jitsukawa, K. Kaneda, *Angew. Chem. Int. Ed.* **2007**, *46*, 3288; *Angew. Chem.* **2007**, *119*, 3352.
[3] W. E. Kaden, T. Wu, W. A. Kunkel, S. L. Anderson, *Science* **2009**, *326*, 826.
[4] J. P. Wilcoxon, P. P. Provencio, *J. Am. Chem. Soc.* **2004**, *126*, 6402.
[5] a) J. P. Bucher, D. C. Douglass, L. A. Bloomfield, *Phys. Rev. Lett.* **1991**, *66*, 3052; b) I. M. L. Billas, A. Châtelain, W. A. de Heer, *Science* **1994**, *265*, 1682.
[6] a) D. Ruiz-Molina, M. mas-Torrent, J. Gómez-Segura, A. I. Balana, N. Domingo, J. Tejada, M. T. Martínez, C. Rovira, J. Veciana, *Adv. Mater.* **2003**, *15*, 42; b) P. Gerbier, N. Domingo, J. Gómez-Segura, D. Ruiz-Molina, D. B. Amabilino, J. Tejada, B. E. Williamson, J. Veciana, *J. Mater. Chem.* **2004**, *14*, 2455; c) N. Domingo, B. E. Williamson, J. Gómez-Segura, P. Gerbier, D. Ruiz-Molina, D. B. Amabilino, J. Veciana, J. Tejada, *Phys. Rev. B* **2004**, *69*, 052405.
[7] a) A. Saywell, G. Magnano, C. J. Satterley, L. M. A. Perdigó, A. J. Britton, N. Taleb, M. del Carmen Giménez-López, N. R. Champness, J. N. O'Shea, P. H. Beton, *Nat. Commun.* **2010**, *1*, 75; b) A. Naitabdi, J.-P. Bucher, P. Gerbier, P. Rabu, M. Drillon, *Adv. Mater.* **2005**, *17*, 1612–1616.
[8] a) D. Aulakh, J. B. Pyser, X. Zhang, A. A. Yakovenko, K. R. Dunbar, M. Wriedt, *J. Am. Chem. Soc.* **2015**, *137*, 9254; b) M. del Carmen Giménez-López, F. Moro, A. La Torre, C. J. Gómez-García, P. D. Brown, J. van Slageren, A. N. Khlobystov, *Nat. Commun.* **2011**, *2*, 407; c) L. Bogani, C. Danieli, E. Biavardi, N. Bendiab, A.-L. Barra, E. Dalcanale, W. Wernsdorfer, A. Cornia, *Angew. Chem. Int. Ed.* **2009**, *48*, 746; *Angew. Chem.* **2009**, *121*, 760.
[9] a) M. Mannini, F. Pineider, C. Danieli, F. Totti, L. Sorace, P. Sainctavit, M. A. Arrio, E. Otero, L. Joly, J. C. Cezar, A. Cornia, R. Sessoli, *Nature* **2010**, *468*, 417; b) M. Mannini, F. Pineider, P. Sainctavit, C. Danieli, E. Otero, C. Sciancalepore, A. M. Talarico, M.-A. Arrio, A. Cornia, D. Gatteschi, R. Sessoli, *Nat. Mater.* **2009**, *8*, 194; c) A. Cornia, M. Mannini, P. Sainctavit, R. Sessoli, *Chem. Soc. Rev.* **2011**, *40*, 3076.
[10] a) F. Grasset, F. Dorson, S. Cordier, Y. Molard, C. Perrin, A.-M. Marie, T. Sasaki, H. Haneda, Y. Bando, M. Mortier, *Adv. Mater.* **2008**, *20*, 143; b) T. Aubert, F. Cabello-Hurtado, M.-A. Esnault, C. Neaime, D. Lebret-Chauvel, S. Jeanne, P. Pellen, C. Roiland, L. Le Polles, N. Saito, K. Kimoto, H. Haneda, N. Ohashi, F. Grasset, S. Cordier, *J. Phys. Chem. C* **2013**, *117*, 20154; c) F. Grasset, F. Dorson, Y. Molard, S. Cordier, V. Demange, C. Perrin, V. Marchi-Artzner, H. Haneda, *Chem. Commun.* **2008**, 4729; d) K. Takao, K. Suzuki, T. Ichijo, S. Sato, H. Asakura, K. Teramura, K. Kato, T. Ohba, T. Morita, M. Fujita, *Angew. Chem. Int. Ed.* **2012**, *51*, 5893; *Angew. Chem.* **2012**, *124*, 5995; e) M. Clemente-León, E. Coronado, A. Forment-Aliaga, P. Amorós, J. Ramirez-Castellanos, J. M. González-Calbet, *J. Mater. Chem.* **2003**, *13*, 3089; f) N. Domingo, E. Bellido, D. Ruiz-Molina, *Chem. Soc. Rev.* **2012**, *41*, 258; g) T. Coradin, J. Larionova, A. A. Smith, G. Rogez, R. Clérac, C. Guérin, G. Blondin, R. E. P. Winpenny, C. Sanchez, T. Mallah, *Adv. Mater.* **2002**, *14*, 896; h) M. Cavallini, J. Gómez-Segura, D. Ruiz-Molina, M. Massi, C. Albonetti, C. Rovira, J. Veciana, F. Biscarini, *Angew. Chem. Int. Ed.* **2005**, *44*, 888; *Angew. Chem.* **2005**, *117*, 910.
[11] X. J. Kong, Y. P. Ren, W. X. Chen, L. S. Long, Z. P. Zheng, R. B. Huang, L. S. Zheng, *Angew. Chem. Int. Ed.* **2008**, *47*, 2398; *Angew. Chem.* **2008**, *120*, 2432.
[12] a) Y.-Z. Zheng, M. Evangelisti, F. Tuna, R. E. P. Winpenny, *J. Am. Chem. Soc.* **2012**, *134*, 1057; b) J.-B. Peng, Q. C. Zhang, X. J. Kong, Y. Z. Zheng, Y. P. Ren, L. S. Long, R. B. Huang, L. S. Zheng, Z. Zheng, *J. Am. Chem. Soc.* **2012**, *134*, 3314; c) J.-B. Peng, Q. C. Zhang, X. J. Kong, Y. P. Ren, L. S. Long, R. B. Huang, L. S. Zheng, Z. Zheng, *Angew. Chem. Int. Ed.* **2011**, *50*, 10649; *Angew. Chem.* **2011**, *123*, 10837.
[13] a) P. H. Lin, T. J. Burchell, R. Clérac, M. Murugesu, *Angew. Chem. Int. Ed.* **2008**, *47*, 8848; *Angew. Chem.* **2008**, *120*, 8980; b) J.-D. Leng, J.-L. Liu, M.-L. Tong, *Chem. Commun.* **2012**, *48*, 5286.
[14] a) A. Baniodeh, C. E. Anson, A. K. Powell, *Chem. Sci.* **2013**, *4*, 4354; b) C. Xiang, S. M. Hu, T. L. Sheng, R. B. Fu, X. T. Wu,

X. D. Zhang, *J. Am. Chem. Soc.* **2007**, *129*, 15144; c) T. N. Hooper, J. Schnack, S. Piligkos, M. Evangelisti, E. K. Brechin, *Angew. Chem. Int. Ed.* **2012**, *51*, 4633; *Angew. Chem.* **2012**, *124*, 4711.
[15] O. Kahn, *Molecular magnetism*, Wiley-VCH, Weinheim, **1993**.
[16] C. Benelli, D. Gatteschi, *Chem. Rev.* **2002**, *102*, 2369.
[17] J. J. Borrás-Almenar, J. M. Clemente-Juan, E. Coronado, B. S. Tsukerblat, *J. Comput. Chem.* **2001**, *22*, 985.
[18] R. Caballol, O. Castell, F. Illas, I. de P. R. Morera, J. P. Malrien, *J. Phys. Chem. A* **1997**, *101*, 7860.
[19] W. Heisenberg, *Z. Phys.* **1928**, *49*, 619.
[20] A. W. Sandvik, *Phys. Rev. B* **1999**, *59*, R14157.
[21] A. F. Albuquerque, F. Alet, P. Corboz, P. Dayal, A. Feiguin, S. Fuchs, L. Gamper, E. Gull, S. Gürtler, A. Honecker, R. Igarashi, M. Körner, A. Kozhevnikov, A. Läuchli, S. R. Manmana, M. Matsumoto, I. P. McCulloch, F. Michel, R. M. Noack, G. Pawłowski, L. Pollet, T. Pruschke, U. Schollwöck, S. Todo, S. Trebst, M. Troyer, P. Werner, S. Wessel, *J. Magn. Magn. Mater.* **2007**, *310*, 1187.
[22] a) Y. Yukawa, G. Aromi, S. Igarashi, J. Ribas, S. A. Zvyagin, J. Krzystek, *Angew. Chem. Int. Ed.* **2005**, *44*, 1997; *Angew. Chem.* **2005**, *117*, 2033; b) S. K. Singh, N. K. Tibrewal, G. Rajaraman, *Dalton Trans.* **2011**, *40*, 10897; c) E. Cremades, S. Gómez-Coca, D. Aravena, S. Alvarez, E. Ruiz, *J. Am. Chem. Soc.* **2012**, *134*, 10532.
[23] a) X. Y. Zheng, S. Q. Wang, W. Tang, G. L. Zhuang, X. J. Kong, Y. P. Ren, L. S. Long, L. S. Zheng, *Chem. Commun.* **2015**, *51*, 10687; b) L. E. Roy, T. Hughbanks, *J. Am. Chem. Soc.* **2006**, *128*, 568.
[24] a) K. K. Nanda, L. K. Thompson, J. N. Bridson, K. Nag, *J. Chem. Soc. Chem. Commun.* **1994**, 1337; b) V. V. Pavlishchuk, S. V. Kolotilov, A. W. Addison, M. J. Prushan, D. Schollmever, L. K. Thompson, E. A. Goreshnik, *Angew. Chem. Int. Ed.* **2001**, *40*, 4734; *Angew. Chem.* **2001**, *113*, 4870.
[25] T. P. M. Alegre, F. G. G. Hernandez, A. L. C. Pereira, G. Medeiros-Ribeiro, *Phys. Rev. Lett.* **2006**, *97*, 4.
[26] CCDC-1436656 contains the supplementary crystallographic data for this paper. These data can be obtained free of charge via www.ccdc.cam.ac.uk/data_request/cif (or from the Cambridge Crystallographic Data Centre, 12 Union Road, Cambridge CB21EZ, UK; fax: (+44)1223-336-033; or deposit@ccdc.cam.ac.uk)..

Received: February 3, 2016
Published online: February 29, 2016

